



LAWRENCE
LIVERMORE
NATIONAL
LABORATORY

Performance measurements on NIF beam lines for future experiments to support polar direct drive

J. K. Crane, B. Kruschwitz, C. Dorrer, S. T. Yang, M. W. Bowers, D. F. Browning, T. S. Budge, D. Canning, J. T. Chou, A. Consentino, J. M. Di Nicola, S. N. Dixit, G. V. Erbert, R. P. Hackel, J. E. Heebner, E. Hill, M. P. Johnston, J. Kelly, J. Kwiatkowski, M. J. Shaw, L. K. Smith, P. J. Wegner, J. Zuegel

January 11, 2016

Inertial Fusion Sciences & Applications
Bellevue, WA, United States
September 20, 2015 through September 25, 2015

Disclaimer

This document was prepared as an account of work sponsored by an agency of the United States government. Neither the United States government nor Lawrence Livermore National Security, LLC, nor any of their employees makes any warranty, expressed or implied, or assumes any legal liability or responsibility for the accuracy, completeness, or usefulness of any information, apparatus, product, or process disclosed, or represents that its use would not infringe privately owned rights. Reference herein to any specific commercial product, process, or service by trade name, trademark, manufacturer, or otherwise does not necessarily constitute or imply its endorsement, recommendation, or favoring by the United States government or Lawrence Livermore National Security, LLC. The views and opinions of authors expressed herein do not necessarily state or reflect those of the United States government or Lawrence Livermore National Security, LLC, and shall not be used for advertising or product endorsement purposes.

Performance measurements on NIF beamlines for future experiments to support polar direct drive

J K Crane¹, B Kruschwitz², S T Yang¹, M Bowers¹, D Browning¹, T Budge¹, D Canning², J Chou¹, A Consentino², J M Di Nicola¹, S Dixit¹, C Dorrer², G Erbert¹, R Hackel¹, J Heebner¹, E Hill², M Johnston¹, J Kelly², J Kwiatkowski², M Shaw¹, L Smith¹, P Wegner¹, J Zuegel²

¹Lawrence Livermore National Laboratory, Livermore, CA, U.S.A.

²Laboratory for Laser Energetics, Rochester, NY, U.S.A.

crane1@llnl.gov

Abstract. We are studying the implementation of polar direct drive (PDD) ignition experiments on the National Ignition Facility (NIF) laser system. Part of this preparation involves testing the performance of the NIF laser system over a broader span of center wavelengths, 3.6 nm, where the laser currently operates and that gain models describe. The temporal shape for the PDD pulses consists of a drive pulse preceded by three lower power “picket pulses”. These picket pulses require a multi-FM sinusoidal phase modulation format with a bandwidth of ~ 200 GHz and a more dispersive grating in the preamplifier module (PAM) for smoothing-by-spectral-dispersion (SSD). In this paper we discuss recent measurements of gain on the NIF laser system over this broader wavelength range. We measured FM-to-AM conversion over the 3.6 nm wavelength. The possibility of pinhole closure due to the larger bandwidth and dispersion associated with multi-FM SSD was studied at LLE on the OMEGA EP laser.

1. Introduction

Laser-driven, inertial confinement fusion requires uniform illumination of a spherical target by x-rays in indirect drive or multiple, high power laser beams in direct drive [1]. The National Ignition Facility[2,3] was designed for indirect-drive fusion where the laser beams are focused into the top and bottom of a cylindrical hohlraum. The hohlraum forms a high temperature x-ray oven that produces the necessary rapid ablative compression of the spherical fuel target [1]. The current cylindrical arrangement of NIF beams can still be used for spherical illumination in polar direct drive (PDD) [4]. PDD requires several modifications to the NIF laser to satisfy the higher degree of illumination uniformity necessary for direct drive. The focus of the laser beams on the spherical fuel target requires a higher degree of smoothing to minimize the speckle present due to spatial coherence. The smoothing of the laser beam on the target surface is accomplished in two ways: rapid dithering of the focal spot in one dimension to smear the speckle pattern[5] produced by the phase plates and splitting each beam into orthogonal polarizations that do not interfere at the target surface. To further increase laser coupling into the target the interacting laser beams are operated at two wavelengths separated by 1.2 nm at the 3rd-harmonic, 351 nm. The large wavelength separation reduces cross-beam energy transfer (CBET) from plasma coupling between laser beams, another source of nonuniformity in the target illumination [4].

PDD will use a special temporal pulse format that consists of three short “picket” pulses that precede a main pulse that is similar to a NIF drive pulse [3]. The picket pulses are phase modulated by the following three rf frequencies, f_n , and modulation depths, $m(f_n)$: $f_1=21.165$ GHz, $m(f_1)=0.45$ radians; $f_2=22.837$ GHz, $m(f_2)=1.04$ radians; $f_3=31.881$ GHz, $m(f_3)=2.07$ radians, producing a bandwidth of ~ 200 GHz. [6,7] These frequencies were determined by modeling the target surface illumination and picking frequencies that did not generate resonances in the surface spatial frequencies that couple to the target [4]. The main drive pulse will be phase modulated at the normal NIF FM frequencies, 3 GHz for SBS suppression and 17 GHz for SSD with $m(3\text{GHz})=5.13$ radians and $m(17\text{GHz})=1.32$ radians.

The frequency modulation is converted to angular dispersion in the far-field by a diffraction grating in the preamplifier module, PAM. For future PDD smoothing experiments we added a 1700 line/mm grating in one NIF PAM to produce $\sim 4X$ the angular dispersion of a 1050 line/mm NIF grating. The line density of the grating yields an angular dispersion for the modulated pulse that is just within the smallest spatial filter pinhole in the NIF laser chain, 150- μ rad radius for the full-size NIF beam.

2. Results

2.1. Energetics

To mitigate the effect of CBET, PDD requires the wavelengths of the upper and lower hemisphere NIF beamlines to be separated by 3.6 nm at 1053 nm. This wavelength offset exceeds the current NIF 1 ω accessible wavelength tuning range of 2 nm (i.e. from 1052 to 1054 nm). To determine the injection energy to the main laser (ML) amplifier required to produce the 16 kJ output energy at these wavelengths, we ran Virtual BeamLine (VBL)[8] simulations of the NIF main laser as a function of injection energy at the Input Sensor Package (ISP) and wavelength. The main laser (ML) amplifiers use combinations of Hoya LHG-8 and Schott LG-770 laser glass, which have gain spectra that fall off differently on either side of gain peak. The gain available at the extreme wavelengths will be constrained by the beamlines with the extreme combinations of laser glasses.

We conducted a series of NIF shots from 4 bundles (i.e. 32 beamlines) at the two chosen offset wavelengths: 1051.5 nm and 1055.0 nm. The initial shot energy was set to 3kJ to minimize amplifier saturation. After each shot, the ML gain in each beamline is computed using the injected energy and loss through the ML. Since slab amplifiers in each beamline are comprised of different mixtures of Hoya LHG-8 and Schott LG-770 glass, regression analysis of gains from the 32 beam-lines with their different slab amplifier composition was carried out to extract the small signal gain of each type of glass separately. Briefly, the ML gain from each beam-line is cast into the following additive form by taking the natural logarithm of the measured gain: $\ln(G) = N_H \times \ln(G_H) + N_S \times \ln(G_S)$, where G is the measured ML gain, $N_{H,S}$ are the number of Hoya and Schott slabs in the beamline respectively, and $G_{H,S}$ are the single pass slab gain of the Hoya and Schott glass slab, respectively.

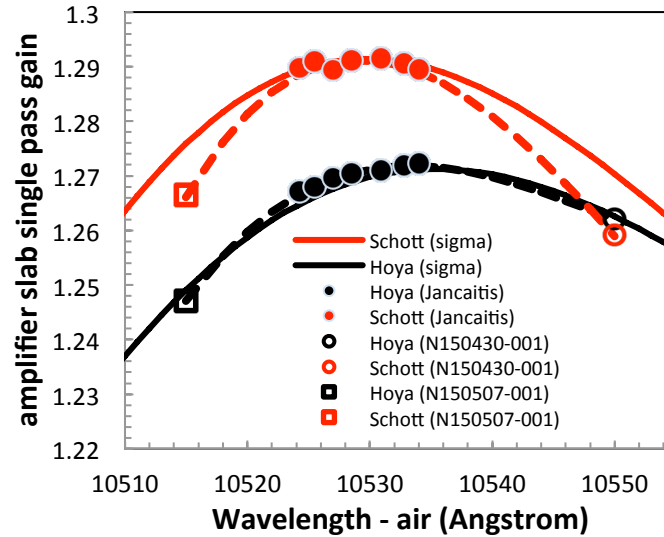


Figure 1. Normalized single pass Hoya and Schott amplifier slab gain as a function of wavelength.

Regression is performed over the 32 beamlines that participated in the shot. The result of the regression analysis is shown in Figure 1, where open circles and squares denote the extracted small-signal gain at the extreme wavelengths. The filled-in circles are small-signal gain measured previously

[9]. Also included in the plot is the gain calculated using emission cross-section values that were measured off-line [10]. These are shown as solid lines. Finally, dashed lines are 3rd order polynomial fits to the measured gains, including gains measured near the peak as well as the ones at the wavelength extremes. As shown in Figure 1, the measured gain, the calculated gain and the polynomial fits all agree well for Hoya glass even at the extreme wavelengths. For Schott glass, however, the measured gain agrees well at the peak but falls faster than the calculation in the wings. We performed a second series of shots on these same 32 NIF beamlines and demonstrated the capability to reach 16 kJ at 1051.5 and 1055 nm.

2.2. Pinhole closure measurements.

With the large spectral dispersion and wide modulation bandwidth inherent in the multi-FM SSD system, the threat of pinhole closure must be considered. Irradiance of the pinhole edge, which increases with both the spectral bandwidth and the dispersion, can generate plasma that expands into the center of the pinhole, causing dangerous modulation of the forward-going beam at the tail end of the pulse [11]. To evaluate the threat of pinhole closure, tests were performed on a beamline of the OMEGA EP laser, which features a very similar architecture to a NIF beamline [12].

No sign of pinhole closure was observed on OMEGA EP up to the maximum 1ω power of 0.6 TW, which is equivalent to 0.3 TW/beam at 3ω , the expected picket power level for Polar Direct Drive picket shots on NIF. Because the OMEGA EP spatial filter, at $f/51$, is significantly faster than the $f/80$ NIF transport spatial filter, the pinhole irradiance on these shots was approximately 2.5 times higher than expected on NIF, and hence this was a conservative test. Irradiance near the edge of the pinhole, as measured by a Schlieren diagnostic, was shown to be significantly below the level required to close our pinhole, according to reference [11]. Figure 2(a) shows the measured irradiance distribution in the output pinhole of OMEGA EP for the 0.6-TW shot, with the pinhole edge indicated by a white circle. Figure 2(b) shows a lineout in the dispersion axis from this shot, with the intensity scaled to the NIF transport spatial filter, and with data from a shot with no dispersed bandwidth shown for reference. The irradiance required to close the pinhole at the end of a 10-ns temporally flat pulse, calculated from reference [8] and scaled to the NIF geometry, is 485 GW/cm² and is indicated by the green line. For ideal alignment into the output pinhole, the measured intensity is approximately 100 times below this closure threshold. Alternatively, the figure shows that pinhole irradiance will be below the closure level over a large pointing tolerance of ± 50 μ rad. Hence, pinhole closure is not a significant threat for the proposed multi-FM SSD system at the power levels being considered for NIF.

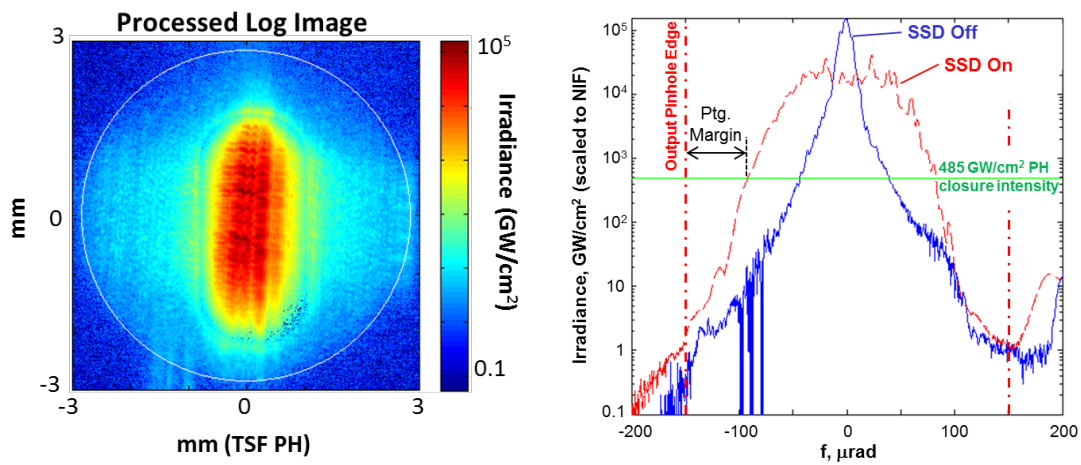


Figure 2. Far-field irradiance measurements from 0.6-TW shots at 1ω , obtained from experiments with multi-FM SSD beam propagation on OMEGA EP: (a) log-scale irradiance distribution in the TSF output pinhole as measured using a Schlieren configuration of the Far-

Field Imaging diagnostic, with the white circle indicating the edges of the 150- μ rad half-angle pinhole; (b) lineout of the irradiance in the dispersion direction, scaled to the NIF transport spatial filter geometry, for the multi-FM SSD system (red) and low-bandwidth system (blue), and with the pinhole edges and pinhole irradiance required for closure of a 10-ns pulse both indicated.

3. Summary and future work

The results presented in this paper demonstrate that we can operate the NIF beamlines at the wavelengths and energy required for future PDD experiments. Measurements on Omega EP at the final filter pinhole edges show that we are a factor of ~ 100 below the irradiance for damage. Recently we installed the multi-FM chassis in the NIF MOR and a 1700 line/mm grating in a NIF PAM and operated a quad of NIF beamlines at the equivalent power level, modulation bandwidth, and angular dispersion necessary to demonstrate the high degree of smoothing required for future PDD experiments. The first of these smoothing experiments will be performed in January 2016 [13].

4. References

- [1] Lindl J 1995 *Phys. of Plasmas* **2**, 3933
- [2] Miller G H *et al* 2004 *Opt. Eng.* **43**, 2841.
- [3] Haynam C A *et al* 2007 *Appl. Opt.* **46**, 3276
- [4] Collins T J B *et al* 2012 *Physics of Plasmas* **19**, 056308
- [5] Rothenberg J E *et al* 1999 *Solid State Lasers for Application to Inertial Confinement Fusion* **3492**, 51
- [6] Kruschwitz B E *et al* 2013 *High Power Lasers for Fusion Research II* **8602**, 86020E-1 (Bellingham, WA SPIE)
- [7] Dorrer C *et al* 2013 *IEEE J. Sel. Topics in Quant. Electr.* **19** 3500112
- [8] Sacks R A *et al* 2015 *High Power Lasers for Fusion Research III* **9345**, 93450M (Bellingham, WA SPIE)
- [9] K. Jancaitis 2013 *Internal LLNL memorandum*.
- [10] R. Page 2006 *Internal LLNL memorandum*.
- [11] Murray J E *et al* 2000 *Appl. Opt.* **39**, 1405
- [12] Kelly J H *et al* 2013 *High Power Lasers for Fusion Research II* **8602**, 86020D-1 (Bellingham, WA SPIE)
- [13] Hohenberger M *et al* 2015 *Physics of Plasmas* **22**, 056308

Acknowledgement

This work was performed under the auspices of the U.S. Department of Energy by the Lawrence Livermore National Laboratory under contract DE-AC52-07NA27344, and at the University of Rochester's Laboratory for Laser Energetics under Award Number DE-NA0001944.